Proceedings of the 27th National and 5th International ISHMT-ASTFE Heat and Mass Transfer Conference
December 14-17, 2023, IIT Patna, Patna-801106, Bihar, India
IHMTC-2023-278

Study of Different Flow Configurations of Radial Flow Annular Reactor for Thermochemical Energy Storage

Ankush Shankar Pujari[1], Rudrodip Majumdar[2], C. Subramaniam[3], Sandip K. Saha[1]

[1]Department of Mechanical Engineering, Indian Institute of Technology Bombay, Mumbai, India
[2]EECP, School of Natural Sciences and Engineering, National Institute of Advanced Studies, IISc Campus, Bengaluru, India
[3]Department of Chemistry, Indian Institute of Technology Bombay, Mumbai, India

ABSTRACT

Thermochemical energy storage is emerging as a promising seasonal thermal energy storage technology. Strontium Bromide has recently become one of the most used salt hydrates for the salt-hydrate and moist air-based open thermochemical energy storage system. This article suggests that radial flow fixed bed reactors offer advantageous configurations owing to their lower pressure drop without compromising thermal performance. Four possible configurations of radial flow fixed bed reactors, Inward flow Π-type, Inward flow Z-type, Outward flow Π-type, and Outward flow Z-type, are analyzed in detail. Energy efficiency, exergy efficiency, pressure drop, and non-dimensional constant named non-uniformity are used as performance metrics for comparing the proposed configurations with four different combinations of flow rates and aspect ratios. It is found that the type of the reactor configuration (Π-type or Z-type) has a negligible impact on the performance, with a maximum change of 4% in the energy efficiency during the hydration phase. The inward and outward flow arrangements exhibit considerable differences in performance, with inward flow having 3.5 times higher exergy efficiency than outward flow. The π-type configuration shows the highest non-uniformity of -0.22 for an aspect ratio of four, with a flow rate of 50 m^3/h.

Keywords: Thermochemical Energy Storage, Radial Flow Annular Reactor, Reactor Configuration, Energy Efficiency, Exergy Efficiency

1. INTRODUCTION

The increasing prices of fossil fuels in the international market and their adverse environmental impacts have resulted in the growing demand for renewable energy to meet the ever-increasing energy demand sustainably. One of the key limitations of globally dominant renewable energy sources (Solar and Wind) lies in the diurnal and seasonal variabilities. Energy storage devices help to overcome this limitation by facilitating energy storage during excess availability and by dispatching the stored energy as per the requirement during the unavailability of harnessable resources. Thermal energy storage can play a crucial role in integrating renewable energy sources, such as solar thermal, for catering to the thermal energy requirements in residential and industrial applications. There are three major storage system types: sensible heat storage, latent heat storage, and thermochemical heat storage, widely used to store solar thermal energy. Sensible and latent heat storage have limitations, such as the requirement of elevated temperature for storage, losses during the storage cycle, and relatively lower energy storage densities. Thermochemical Energy Storage (TCES), with much higher storage densities and theoretically negligible energy losses, provides an attractive option for long-term (seasonal) energy storage at normal temperatures. Over the past two decades, research efforts have focused on characterizing thermochemical materials and analyzing the performance of TCES systems under various operating strategies. TCES systems can be operated as open or closed systems using moist air or pure water vapour. The salt hydrate-based solid-gas reactions in an open system have received ample attention from researchers for residential applications. It facilitates ease of operation with moist air as the reacting and heat transfer fluid. The heated air can be used for household purposes such as space heating. One of the critical limitations of such an open system with a fixed bed reactor is the pressure drop across the reactor bed and the requirement of an external energy source (electrical or mechanical) for providing the required flow work.

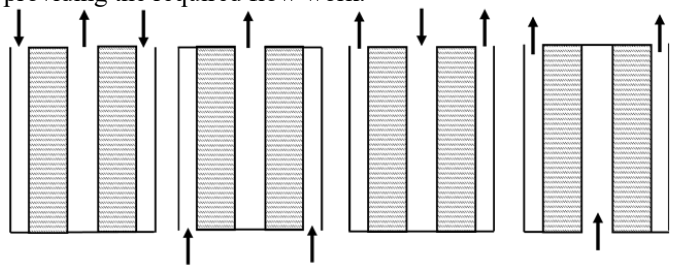

Figure 1: Reactor configurations for radial flow (a) Inward π-type, (b) Inward Z-type, (c) Outward π-type, (d) Outward Z-type

Radial Flow Fixed Bed Reactors (RFBR) with annular reactive beds are promising solutions for reducing the auxiliary power requirement. It offers less pressure drop and requires

lesser auxiliary power, while there is no compromise on the system's performance regarding thermal power output. Two configurations are possible with the RFBR based on air connection strategies, the Z-type and Π -type. Further, these two configurations can be operated with either radially inward or outward flow directions, allowing four possible operating configurations, as shown in **Figure 1**.

2. LITERATURE REVIEW AND OBJECTIVE

Lele and Tamba [1] explained the implementation of TCES systems for household applications. Strontium Bromide Hexahydrate ($SrBr_2.6H_2O$) is one of the most popular TCES materials [1,2,3] owing to its high energy storage density (theoretical value of 628 $kWh.m^{-3}$). It has a dehydration temperature of 70-80 °C (equilibrium water vapour pressure equal to 7600 Pa to 15000 Pa) and a hydration temperature of 35 °C (equilibrium water vapour pressure equal to 500 Pa). Therefore, it makes the TCES suitable for charging with a solar air heater and discharging heat to cater to space heating applications. The dehydration (charging) process converts Strontium Bromide Hexahydrate ($SrBr_2.6H_2O$) into Strontium Bromide Monohydrate ($SrBr_2.H_2O$). The reverse process, called hydration (discharging), releases the heat upon absorbing the water vapour molecules, converting $SrBr_2.H_2O$ into $SrBr_2.6H_2O$ in the process. The hexahydrate form thus produced undergoes dehydration during the next cycle. This is the operating philosophy for the consecutive cycles. **Equation (1)** represents the hydration-dehydration reaction where the heat of the reaction is equal to 337 kJ/mol.

$$SrBr_2.H_2O_{(s)} + 5H_2O_{(g)} \rightleftarrows SrBr_2.6H_2O_{(s)} + Heat \qquad (1)$$

A detailed methodology has been presented by Abedin et al. [4] for calculating the energy and exergy efficiency of the open and closed TCES systems, including a detailed performance analysis of the $SrBr_2.6H_2O$-based open TCES systems. The approach for analyzing energy and exergy efficiencies proposed by Abedin et al. [4] is implemented in the present study to compare the performance of different flow configurations (see **Figure 1)**. The reactor design and working parameters affect the reaction advancement within the reactor, thereby impacting the system's thermal performance. A detailed parametric study is presented by Hawwash et al. [5], explaining the effect of reactor design on the performance of the TCES system. Li [6] and Gaganova et al. [7], in their respective articles on radial flow fixed bed reactors (RFBR) for catalytic reactions, explained the various issues affecting the reactor performance, such as catalyst settling, flow bypassing, and catalyst pinning. Some of the essential aspects of RFBR configuration are highlighted, including lower pressure drop and the potential to reduce auxiliary power requirements in industrial applications. Xing et al. [8] analyzed the effect of the opening strategy and opening rate of the center pipe and the annular channel on the flow distribution uniformity within the reactor bed. Using numerical simulations, the analysis showed the effectiveness of a three-stage opening strategy at different air flow rates and widths of the outer annular channel. Lesser non-uniformity was observed for the configuration with the ratio of the center pipe cross-sectional area to the outer annular air channel cross-sectional area being equal to unity or slightly greater than unity. Kareeri et al. [9] presented a detailed comparison of the Z-type and Π-type configurations with inward (Centripetal, CP) and outward (Centrifugal, CF) flow arrangements in the RFBR. The study highlights the effect of pressure drop within the air channels based on non-uniformity in the flow distribution across the length of the reactor. The reactor analyzed by Kareeri et al. has an aspect ratio of 7.5. It is observed that the higher length and higher aspect ratio lead to a higher pressure drop within the air channel, producing more non-uniformity in flow distribution.

The present study is a continuation of the published work pertinent to the comparative analysis of radial flow reactors (RFBR) and conventional axial flow cylindrical or parallelopiped reactors [10]. The present study aims to understand the possible maldistribution of the flow within the reactor bed designed for the TCES system with different possible flow configurations explained in **Figure 1**. Detailed performance analysis has been conducted to identify the configuration with better performance and optimum working parameters.

3. 2D AXISYMMETRIC NUMERICAL MODEL

A two-dimensional (2D) axisymmetric model is used to simulate the hydration and dehydration processes in the COMSOL Multiphysics v5.6 [9-12] environment for the proposed system configurations. The developed numerical model uses the Darcy-Brinkman equation coupled with heat transfer and moisture transport in the porous reactive bed. The source terms are defined using the first-order reaction kinetics equation, utilizing the reaction constant calculated based on the Arrhenius Equation for the hydration-dehydration process involving different Strontium Bromide hydrates [2,3]. For the hydration process, the inlet condition comprises a temperature of 285 K with 60% relative humidity (RH), whereas the inlet condition for the dehydration process comprises temperatures of 343 K and 3% RH.

The essential properties affecting the flow through porous media are provided in **Table 1**. The properties from **Table 1** are applied to the hexahydrate (hydrated) and monohydrate (dehydrated) salt. For intermediate reaction advancement, properties are averaged based on the volume percentage of the hydrated and dehydrated salt. The porosity and permeability of the bed at the intermediate stages of the reaction are calculated using the simple volume averaging for the hydrated and dehydrated salt in the partially hydrated salt bed [11].

Table 1: Properties of porous reactive bed for the proposed analysis [3]

Properties	Value
Porosity of hydrated salt (-)	0.38
Porosity of dehydrated salt (-)	0.68
Permeability of the air in hydrated salt (m^2)	5.9×10^{-11}
Permeability of the air in dehydrated salt (m^2)	5.7×10^{-10}

Figure 2 shows the axisymmetric numerical domain with different dimensions used in the modeling. The inlet and outlet boundary conditions are applied according to the configuration. The detailed verification and grid independence study for the

numerical model are presented in a previous study presented by Pujari et al. [11]. Global reaction advancement and temperature distribution are verified with the results published by Mukherjee et al. [3], and pressure drop is verified against analytical calculations. Numerical simulation results show good agreement against the values used for verification. Grid independence study is conducted with three different grid sizes (coarse, fine, and extremely fine) available in the simulation tool.

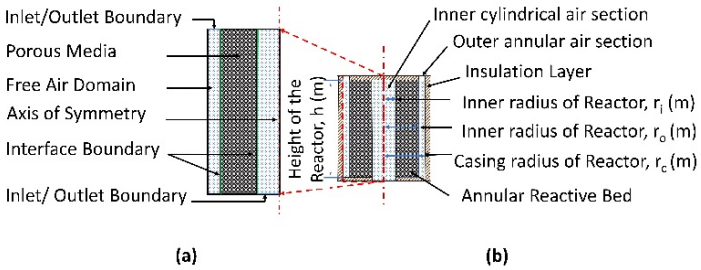

Figure 2: Schematic representation and details of (a) computational domain for axisymmetric model and (b) 2D section view of the reactor geometry

The dimensions of the reactor bed used for the proposed study are presented in **Table 2**. Two different configurations with aspect ratios of 1 and 4, respectively, are studied, where the aspect ratio is defined as the ratio of the length of the reactor bed to the difference between the inner and outer diameters of the reactor. Energy storage capacity defines the volume of the reactive bed and is constant for all the configurations.

Table 2: Physical dimensions for the reactor under consideration for the proposed study

Parameter	Value for AR 1	Value for AR 4
Energy Storage Capacity (kWh)	10	10
Salt Volume (m^3)	0.0258	0.0258
Inner Diameter of Reactor Bed (r_i) (m)	0.05	0.05
Outer Diameter of Reactor Bed (r_o) (m)	0.18	0.126
Outer Casing Diameter (r_c) (m)	0.19	0.14
Height of the Reactor bed (h) (m)	0.26	0.61

Four combinations are defined with two different airflow rates and two aspect ratios which are compared for the Z-type and Π-type flow configurations with inward and outward flow directions. The chosen four combinations of airflow rates and aspect ratios are provided in **Table 3**. Detailed simulations are conducted for the discharging (hydration) and the charging (dehydration) processes.

Table 3: Four different cases with corresponding flow rates and aspect ratios

Configuration	Air Flow Rate	Aspect Ratio
15CMH AR01	15 m^3/h	01
15CMH AR04	15 m^3/h	04
50CMH AR04	50 m^3/h	04
50CMH AR01	50 m^3/h	01

Energy and exergy efficiencies are used as the performance metrics to compare the performance of the proposed four configurations. Pressure drops within the air channel and across the reactor bed for one case (50CMH AR01) are analyzed from the simulation data and are compared to understand the effect of flow configuration and direction. Further, the non-uniformity values are calculated based on the pressure drop across the reactor bed as a measure of the extent of maldistribution of the flow across the length of the reactor.

4. RESULTS AND DISCUSSION

4.1 Exergy and Energy Efficiency

This section presents the energy and exergy efficiencies of the TCES system for different reactor configurations. Along with the effect of flow configuration (Π vs. Z), the effect of flow direction (inward vs. outward), the effect of aspect ratio, and the effect of flow rate are discussed. **Figure 3** represents the performance of the hydration (discharging) process in terms of energy efficiency (**Figure 3(a)**) and exergy efficiency (**Figure 3(b)**). **Figure 4** represents the performance of the dehydration (charging) process in terms of energy and exergy efficiencies (**Figures 4(a)** and **4(b)**), respectively.

The exergy efficiency highly depends on the pressure drop across the reactor bed, which is highly affected by the inward or outward flow direction. Thus, exergy efficiency remains nearly unaffected by the configurational choice, with the maximum difference being less than 1% and highly dependent on flow direction. **Figure 3** and **Figure 4** show a considerable difference between the performances of the inward and outward flow configurations, irrespective of the rector type (Z-type or Π-type). For any specific aspect ratio and flow rate, the inward flow gives better exergy efficiency than the outward flow, which is attributed to the lower pressure drop across the rector for inward flow. In the case of 15CMH AR01, the hydration phase exergy efficiency of the inward flow is 3.5 times higher than the outward flow counterpart (absolute values of 0.19 and 0.04, respectively). The energy efficiencies for the outward flow nearly remain constant for changing aspect ratios. Energy efficiency is higher for the outward flow configuration at higher aspect ratios compared to the inward flow counterpart. This is mainly attributable to low nonuniformity in the flow, which is discussed in the following sections.

The Π-Inward and Z-Inward configurations show a maximum of 2.7% difference in energy efficiency for the hydration process and 0.9% for the dehydration process. The Π-Outward and Z-Outward flow configurations show a maximum difference of about 8% in exergy efficiency in the case of hydration (absolute values of 0.04 and 0.05, respectively) and 0.16% in energy efficiency during hydration (absolute values of 0.50 and 0.49, respectively).

Reactors with an aspect ratio of 4 show better exergy efficiency during hydration and dehydration due to lesser pressure drop across the reactor bed attributable to the lower radial thickness associated with a higher reactor aspect ratio. A higher aspect ratio leads to a lower residence time for the reacting fluid within the reactor bed, thereby reducing energy efficiency. The lower flow rate of 15 m^3/h shows better energy and exergy efficiencies due to lower pressure drop and better

energy transfer between the reacting fluid and the reactor bed, owing to higher residence time.

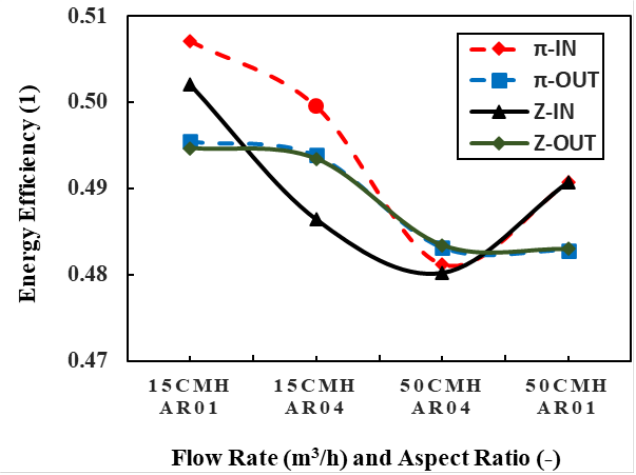

Figure 3: Performance of the hydration process for various configurations (a) Energy Efficiency and (b) Exergy Efficiency

4.2 Pressure drop and non-uniformity in the flow

Compared to that across the whole reactor, the pressure drop within the air channel plays a crucial role in the flow distribution and performance of the system. **Table 4** explains the pressure drop for the 50CMH AR01 case with a flow rate of 50 m^3/h and an aspect ratio equal to one.

Table 4: Pressure drop across the reactive bed and in the inner and outer air sections (For the Hydration Process with 50CMH AR01 case)

Pressure Drop (Pa)	Inlet to Outlet	Across Reactor	Inner channel	Outer Channel
Π -In	1575	1344	103	152
Π - Out	2544	2241	181	147
Z-In	1677	1341	208	251
Z-Out	2649	2241	285	250

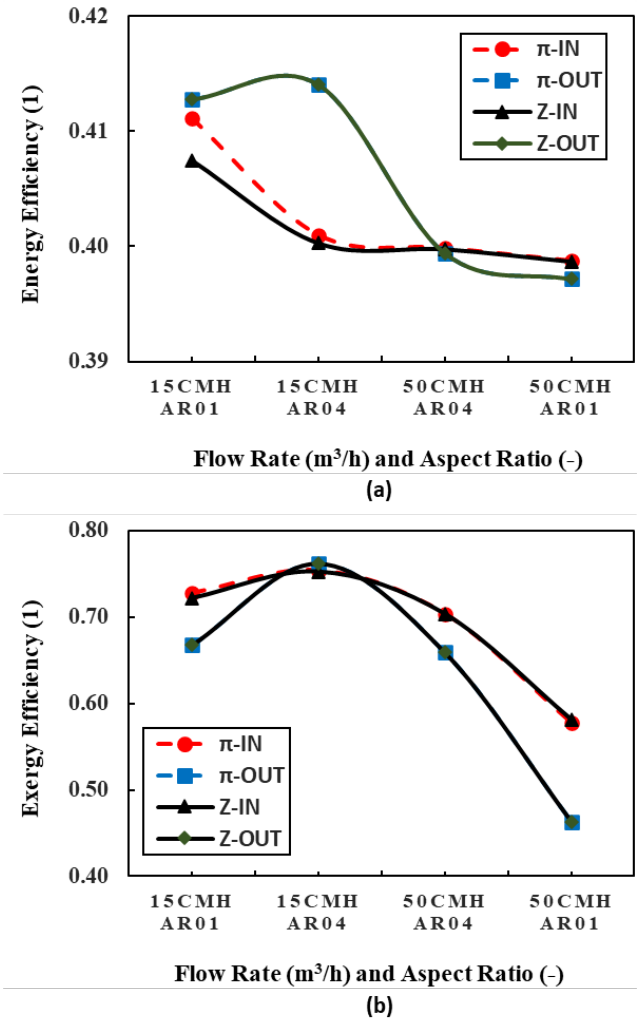

Figure 4: Performance of the dehydration process for various configurations (a) energy efficiency and (b) exergy efficiency

There is a considerable difference between pressure drop values of inward flow and outward flow configurations (nearly 60% higher for outward flow). Still, the pressure drop is nearly the same with a specific flow direction for both Π-type and Z-type reactors.

It is evident from the better exergy efficiency of the inward flow configuration that the higher-pressure drop reduces the exergy efficiency of the outward flow counterpart, as presented in **Figures 3(b)** and **4(b)**. Similar pressure drop profiles are observed for the other flow rates and aspect ratios. **Figure 5** shows the time-averaged pressure distribution within the inner and outer channels of the reactor bed along its length during the hydration process for the 50CMH AR01 case. To simplify the presentation, non-dimensional length (NDL) is used instead of absolute length, with the value ranging from zero to one, with NDL=0 representing the bottom of the reactor bed and NDL=1 indicating the top of the rector bed.

For Π-Inward flow configuration, air enters the outer channel at NDL = 1 and flows towards NDL = 0 through the same channel, thus exhibiting an increase in pressure from NDL

= 0 to 1. For the inner channel, the outlet is at NDL = 1, and pressure decreases from NDL 0 to 1. The pressure drop in the air channel causes the maximum radial pressure difference at NDL = 1 and the minimum radial pressure difference at NDL = 0, as shown in **Figure 5(a)**. A similar phenomenon is observed for the Π-Outward flow configuration, with pressure increasing in the inner channel and decreasing in the outer channel from NDL = 0 to 1. Therefore, it leads to the maximum radial pressure drop at NDL = 1 and the minimum pressure drop at NDL = 0 for the Π-Outward configuration, as shown in **Figure 5(b)**. Also, outward flow exhibits a higher pressure drop than inward flow configuration, which is attributed to the outward movement of the reaction front leading to variation in the porosity of the bed, as explained in detail in the previous studies by Pujari et al. [11].

In the case of Z-Inward flow configuration, air enters the outer channel at NDL = 1, and thus, air pressure in the outer channel decreases from NDL = 1 to 0. The outlet is connected to the inner channel at NDL = 0, and therefore, the pressure within the inner channel increases from NDL = 0 to 1. Similarly, in the case of Z-Outward flow configuration, pressure in the inner and outer channels decreases from NDL=0 to 1. The results show that the radial pressure difference for the Z-type configuration is nearly constant with respect to the height of the reactor, with <3% variation for inward flow and <1.5% variation for outward flow, as shown in **Figures 5(c)** and **5(d)**. From the pressure profiles, it is evident that the Π-type reactor exhibits a higher extent of non-uniformity in the radial pressure drop, indicating a greater extent of maldistribution of the reacting fluid (Moist air) along the reactor height.

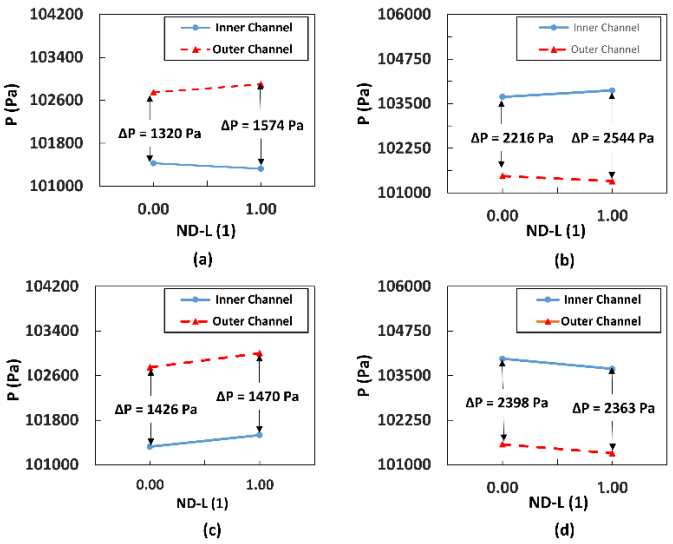

Figure 5: Time-averaged pressure (P) distribution within inner and outer air sections along the non-dimensional length (ND-L) for the Hydration Process with 50MPH AR01 case (a) π-Inward, (b) π-Outward, (c) Z-Inward, (d) Z-Outward

A non-dimensional quantity called as ***non-uniformity*** is used to quantify the extent of axial maldistribution of the radial flow. The non-uniformity is given by **Equation 2** [9]:

$$non-uniformity = \left(1 - \sqrt{\frac{Radial\ \Delta P\ at\ reactor\ top}{Radial\ \Delta P\ at\ reactor\ bottom}}\right) \quad (2)$$

Table 5 presents the calculated values of non-uniformity for all four configurations and the chosen four combinations of flow rates and aspect ratios. A negative sign indicates a higher pressure drop at the top of the reactor, which further leads to a higher flow rate and reaction rate in the upper section of the reactor. A value close to zero indicates better uniformity of the flow across the reactor height. The Z-type configurations exhibit lesser non-uniformity due to the uniform radial pressure drop obtained for both inward and outward flow configurations, as can also be seen from **Figures 5(c)** and **5(d)**. It also establishes that the combination of a lower aspect ratio and a lower flow rate offers lower non-uniformity compared to the combination of a higher aspect ratio and a higher flow rate, with other parameters remaining unchanged. The outward flow arrangement exhibits a lower non-uniformity than the inward flow counterpart, leading to a better flow distribution and utilization of the reactor bed.

Table 5: Non-uniformity in the flow during the Hydration Process for chosen configurations.

	Π - Inward	Π - Outward	Z- Inward	Z- Outward
15CMH AR01	-0.03	-0.03	-0.01	0.002
15CMH AR04	-0.09	-0.07	-0.04	-0.004
50CMH AR04	-0.22	-0.18	-0.09	-0.01
50CMH AR01	-0.09	-0.07	-0.02	-0.01

5. CONCLUSIONS

Amongst the identified four reactor configurations, there is not much difference in the performance of Π-type and Z-type reactors for a particular flow arrangement (radially inward or outward). However, a significant difference in the performance is observed when the comparisons are drawn between the radially inward and outward flow arrangements. For a reactor aspect ratio of 1 and working fluid flow rate of 15 m^3/h, the hydration phase exergy efficiency of the inward flow is 3.5 times higher than the outward flow counterpart. A lower flow rate shows better performance for the hydration and dehydration processes, irrespective of the system configuration. Pressure distribution shows that the Z- configuration has a more uniform radial pressure drop across the reactor bed height as against the Π- configuration. The Π-configuration exhibits the maximum non-uniformity for the 50CMH AR04 case. This indicates that the Π-configuration, accompanied by the combination of a higher aspect ratio and a higher flow rate, leads to higher non-uniformity, and less efficient reactive bed utilization.

ACKNOWLEDGEMENTS

The authors acknowledge the financial support from the SERB, DST, INDIA, through grant no. CRG/2021/000221 to carry out this work.

REFERENCES

[1] Fopah-Lele, J.G. Tamba, A review on the use of $SrBr_2 \cdot 6H_2O$ as a potential material for low temperature energy storage systems and building applications, Solar Energy Materials and Solar Cells. 164 (2017) 175–187.

[2] B. Michel, P. Neveu, N. Mazet, Comparison of closed and open thermochemical processes, for long-term thermal energy storage applications., Energy. 72 (2014) 702–716.

[3] A. Mukherjee, R. Majumdar, S.K. Saha, L. Kumar, C. Subramaniam, Assessment of open thermochemical energy storage system performance for low temperature heating applications, Appl Therm Eng. 156 (2019) 453–470. DOI: 10.1016/j.applthermaleng.2019.04.096

[4] A.H. Abedin, M.A. Rosen, Closed and open thermochemical energy storage: Energy- and exergy-based comparisons, Energy. 41 (2012) 83–92.

[5] A.A. Hawwash, H. Hassan, K. El, Impact of reactor design on the thermal energy storage of thermochemical materials, Appl Therm Eng. 168 (2020).

[6] J.C.H. Li, Radial-flow packed-bed reactors, in: Ullmann's Encyclopedia of Industrial Chemistry, Wiley, (2021) 1–32.

[7] V.N. Gaganova, S.S. Lachinov, N.S. Torocheshnikov, Prospects for the use of radial ammonia synthesis columns, Tr. Mosk. Khim-Tekhnol. Inst., 65 (1970) 132-5.

[8] Y. Xing, C. Zhang, H. Wang, Z. Li, Y. Liu, Airflow distributions in a z type centripetal radial flow reactor: effects of opening strategy and opening rate, Processes. 10 (2022).

[9] A.A. Kareeri, H.H. Zughbi, H.H. Al-ali, Simulation of flow in a radial flow fixed bed reactor (RFBR), (2015).

[10] A.S. Pujari, R. Majumdar, S.K. Saha, Thermochemical energy storage using radial flow annular reactor for attaining lower pressure drop (Paper No. ENFHT 170), Proceedings of the 8th World Congress on Momentum, Heat and Mass Transfer (MHMT'23), Lisbon, Portugal, March 26 – 28, (2023). DOI: 10.11159/enfht23.170

[11] A.S. Pujari, R. Majumdar, S.K. Saha, C. Subramaniam, Annular vertical cylindrical thermochemical storage system with innovative flow arrangements for improved heat dispatch towards space heating requirements, Renewable Energy 217, (2023). DOI: 10.1016/j.renene.2023.119168

[12] A.G. Dixon, D. Polcari, A. Stolo, M. Tomida, COMSOL Multiphysics ® simulation of flow in a radial flow fixed bed reactor (RFBR), (2015).